Experimental investigation of flame pattern transitions in a heated radial micro-channel

Aiwu Fan [a,*], Kaoru Maruta [b], Hisashi Nakamura [b], Wei Liu [a]

[a] School of Energy and Power Engineering, Huazhong University of Science and Technology, 1037 Luoyu Road, Wuhan 430074, China
[b] Institute of Fluid Science, Tohoku University, 2-1-1 Katahira, Aoba-ku, Sendai, Japan

ABSTRACT

Flame pattern transitions of CH_4/air mixture were experimentally investigated in a radial micro-channel. These transitions were triggered by a variation in the mixture equivalence ratio or inlet mixture velocity. The transition processes were recorded with a high-speed digital video camera. From the movies, it is shown that the mechanisms responsible for these transitions could be classified into two: (1) transitions from a stable circular flame to a traveling flame, and from a traveling flame to single or double Pelton-like flames were due to local extinction in the flame front, and (2) transition from an unstable circular flame to a spiral-like flame was due to local splitting of the flame front. Numerical simulation of the isothermal flow demonstrated that flow field is symmetric and steady when the inlet velocity is small, but it grows asymmetric and unstable at large inlet velocities. The asymmetric and unstable flow field is expected to be the possible reason for the local splitting of flame front. On the other hand, flame is noted to be quenched near the top wall surface. These two reasons are expected to induce the transition from an unstable flame to a rotating spiral-like flame.

© 2012 Elsevier Ltd. All rights reserved.

1. Introduction

With the rapid development of MEMS technology, there is an urgent demand for micro-power generation devices and systems. As the electrochemical batteries have disadvantages of a short life span, long recharging periods and low energy densities, combustion-based power sources are considered to be potential alternatives to conventional batteries due to the much higher energy densities of hydrocarbon fuels [1,2]. Therefore, micro- and meso-scale combustions have received great attention in the past decade [3–33]. However, the increased heat losses due to large surface area-to-volume ratio and the wall radical quenching make it difficult to sustain a stable flame under small scales [1–5]. Numerical analyses demonstrated that heat conduction in the solid walls has a great effect on flame stability in micro-channels [6,7]. Heat recirculation is frequently adopted in the design of micro-combustors. The "Swill roll" combustor is a well-known example and it has already been implemented to stabilize flames in micro- and meso-scales burners [8–12]. Other researchers also developed different approaches to stabilize flame in micro-combustors [13–16].

Many contributions have been made to understand fundamentals of combustion at reduced scales with heat recirculation. To facilitate direct observation of the flame dynamics in micro-channels, Maruta et al. [17,18] used a micro-tube made of transparent quartz. The combustion chamber is optical accessible and thus the detailed flame structures and dynamics can be identified with an image-intensified high-speed video camera. In their experiments, in order to simulate the heat-recirculating effect like the "Swiss roll" combustor, a wall temperature profile in the flow direction was generated with an external heat source before the introduction of fuel. They found that stable flames occurred at high and low inlet mixture velocities. When the inlet mixture velocity was decreased or increased to a moderate value, transition from stable flame to unstable flame propagation modes occurred. Those combustion waves include the flame with repetitive extinction and ignition (FREI). It was also demonstrated that the flame location versus inlet mixture velocity exhibited an S-shaped curve [18,19]. This phenomenon stimulated the passions of many other researchers [20–27].

Following the idea of Maruta et al. [17,18], Kumar et al. [28–30] discovered a variety of non-stationary flame patterns of CH_4/air mixtures in a heated radial micro-channel, such as the traveling flame, rotating Pelton-like flame, spiral-like flame, and so on. Later, Fan et al. [31] carried out a 2D numerical simulation of combustion in this configuration using a global one-step Arrhenius reaction

* Corresponding author. Tel.: +86 27 87542618; fax: +86 27 87540724.
 E-mail address: faw@mail.hust.edu.cn (A. Fan).

model and did not consider flow field. Fortunately, single and double Pelton-like flames were successfully reproduced. However, this model did not work for the spiral-like flame. Based on systematic experiments, flame pattern regime diagrams of the radial channel were obtained [32]. Those diagrams present a clear overview of the relation between each flame pattern and the experimental parameters, such as the inlet mixture velocity, mixture equivalence ratio and channel gap distance. Some important information can be got from those regime diagrams, e.g., an increase of the channel gap distance does not mean a wider stable combustion region could be obtained. In Ref. [33], Fan et al. further investigated the effect of wall temperature level on flame stability in the radial channel. The experimental results indicated that the region occupied by the stable flame became much larger at low inlet velocities for a higher wall temperature level; however, flame instability showed little improvement in the high inlet velocity region.

An overview of the experimental and numerical results in [31–33] shows that the Pelton-like flame and traveling flame are more affected by heat losses; while the spiral-like flame may have a close relation to the instability of the flow field. On the other hand, as can be seen from the flame pattern regime diagrams [32], transitions between adjacent flame patterns can be realized through a variation of the mixture equivalence ratio or inlet mixture velocity. These informations drop us a hint that flame pattern transitions might shed some light onto the possible underlying physics of flame pattern formations in the heated radial channel. Also, more attention should be paid to the effect of flow instability. For this, we conducted experimental investigations on several flame pattern transitions: (1) from a stable circular flame to a traveling flame, (2) from a traveling flame to single and double Pelton-like fames, and (3) from an unstable flame to a spiral-like flame. Investigations on the flow field will also be performed through numerical simulation.

2. Experimental setup and method

The experimental setup is identical to that used in our previous study [28–33]. A schematic diagram of the experimental setup is shown in Fig. 1. Two quartz discs (Ø50) were maintained parallel to form a radial channel. A delivery tube of a 4.0-mm diameter was connected to the center of the top disk. A cooling system was utilized to maintain the upstream temperature of the incoming gas at ~300 K. The gap distance of the two disks is adjustable. Before the supply of methane gas fuel, the radial channel was heated by a porous metal burner from the bottom and a cold air flow was fed into the channel. After ~30 min, a steady wall temperature profile was generated to simulate the practical heat-recirculating-type micro combustors, as shown in Fig. 2. This approach was also
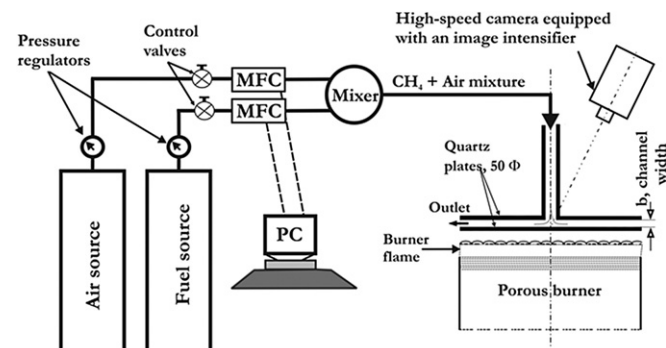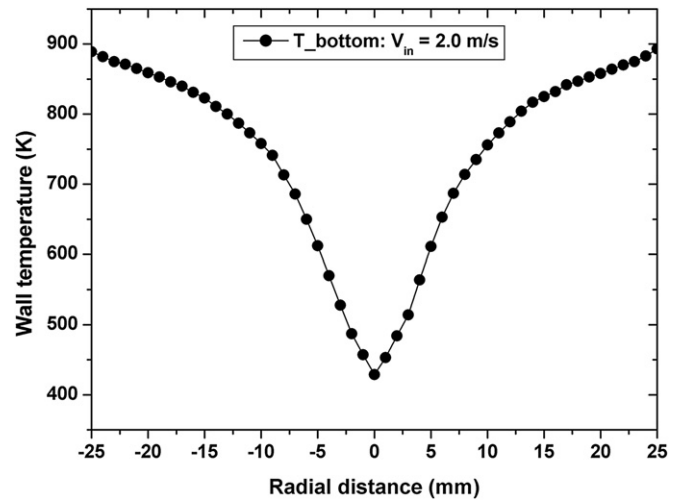
Fig. 2. Measured temperature profile of the bottom plate when $V_{in} = 2.0$ m/s.

employed in the series of previous studies [28–33]. The equivalence ratio and flow velocity were adjusted by the mass flow controller, which was linked with a personal computer (PC). A high-speed digital video camera was used to make movie recording of the flame pattern transition processes. A rate of 250 frames per second (fps) was adopted for all the experiments. The high-speed video camera was also controlled through the same PC. All the operations on it were done by clicking the mouse. When the flame pattern transition experiment is started, we first change the equivalence ratio/flow velocity through the PC, and then quickly push down the "record" button on monitor software of the high-speed video camera. The transition process can be clearly shown on the screen of the PC. When the transition process is finished, we shut down the high-speed camera. This whole process is accomplished in less than 8 s. The transition processes are even much shorter. For example, we will show 18 sequential frames to demonstrate the whole transition process from a stable circular flame to a traveling flame, which means the transition process takes place in less than 0.072 s. Thus, the effect of wall temperature variation could be neglected in such a short time.

The experiments were conducted under the guidance of the flame pattern regime diagrams presented in our previous paper [32]. In that work, the intervals for the inlet mixture velocity and mixture equivalence ratio were 0.5 m/s and 0.05, respectively. Thus, transitions in the present study were realized through changing the mixture equivalence φ, by 0.05, or the inlet mixture velocity, V_{in}, by 0.5 m/s. For an easy understanding by the readers, the conditions that triggered those transitions are listed in Table 1. The gap distances of the radial channel used in the experiments were 2.0 and 3.0 mm.

Fig. 1. Schematic diagram of the experimental setup.

Table 1
Conditions used in the experiments of flame pattern transitions.

	Conditions	Results
I	$b = 2.0$ mm, $V_{in} = 4.0$ m/s, φ increases from 1.20 to 1.25	Transition from a stable circular flame to a traveling flame
II	$b = 2.0$ mm, $V_{in} = 3.5$ m/s, φ increases from 1.25 to 1.30	Transition from a traveling flame to double Pelton-like flames
III	$b = 2.0$ mm, $V_{in} = 4.0$ m/s, φ increases from 1.25 to 1.30	Transition from a traveling flame to single Pelton-like flame
IV	$b = 3.0$ mm, $\varphi = 0.95$, V_{in} increases from 5.5 m/s to 6.0 m/s	Transition from an unstable circular flame to a spiral-like flame

3. Experimental results

3.1. Transition I: from a stable circular flame to a traveling flame

This flame pattern transition took place in the radial micro-channel with a gap distance of 2.0 mm. First, we introduced a methane/air mixture of $V_{in} = 4.0$ m/s and $\varphi = 1.20$. A stable circular flame appeared. Soon after, we changed the equivalence ratio from 1.20 to 1.25. The transition from a stable circular flame to a traveling flame occurred and the whole process was recorded by a high-speed digital video camera, as shown in Fig. 3(a)–(r).

From Fig. 3(a), it is noted that although it is a stable circular flame, the luminosity of the flame front is not uniform. It means that there are some weak parts in the flame front. When the mixture equivalence ratio was increased by 0.05, those parts became even weaker and local extinction occurred soon after, as shown in Fig. 3(b) and (c). Then, the circular flame front was broken (see Fig. 3(d)). However, as the broken gap was not so broad, the leaked fuel–air mixture was reignited by the two tips of the flame. As a result, the flame front recovered to an entire cycle again (see Fig. 3(e) and (f)). Nevertheless, as time passed, the reaction of the richer mixture grew even weaker. Flame at that location became increasing darker and were extinguished again (see Fig. 3(g)–(k)). At the moment of Fig. 3(l), the leaked fuel–air mixture was ignited at a location of larger radius. This Pelton-like flamelet then ignited the mixture close to it and propagated to the opposite side (see Fig. 3(m)–(o)). Meanwhile, another flamelet with an identical geometry was also generated at the opposite flame end and emerged with the coming one (see Fig. 3(p)). From then on, the process from Fig. 3(l) to (p) repeated (see Fig. 3(q) and (r)) and the traveling flame was formed.
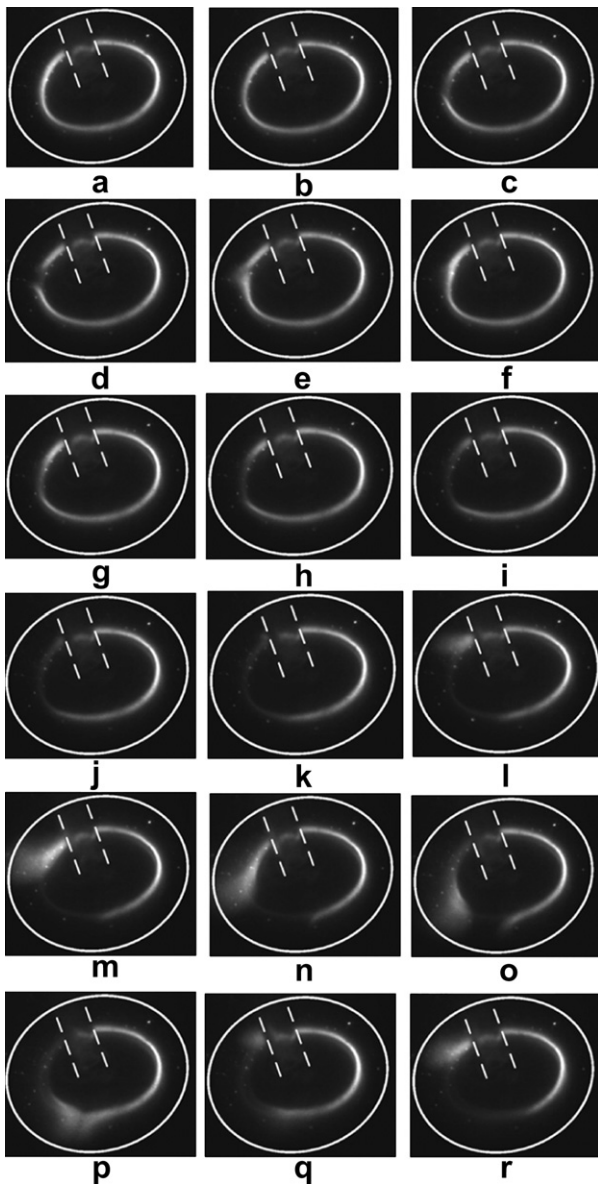
Fig. 3. Sequential frames of the transition process from a stable circular flame to a traveling flame. The gap distance of the radial channel $b = 2.0$ mm, inlet mixture velocity $V_{in} = 4.0$ m/s, and the mixture equivalence ratio φ was changed from 1.20 to 1.25.
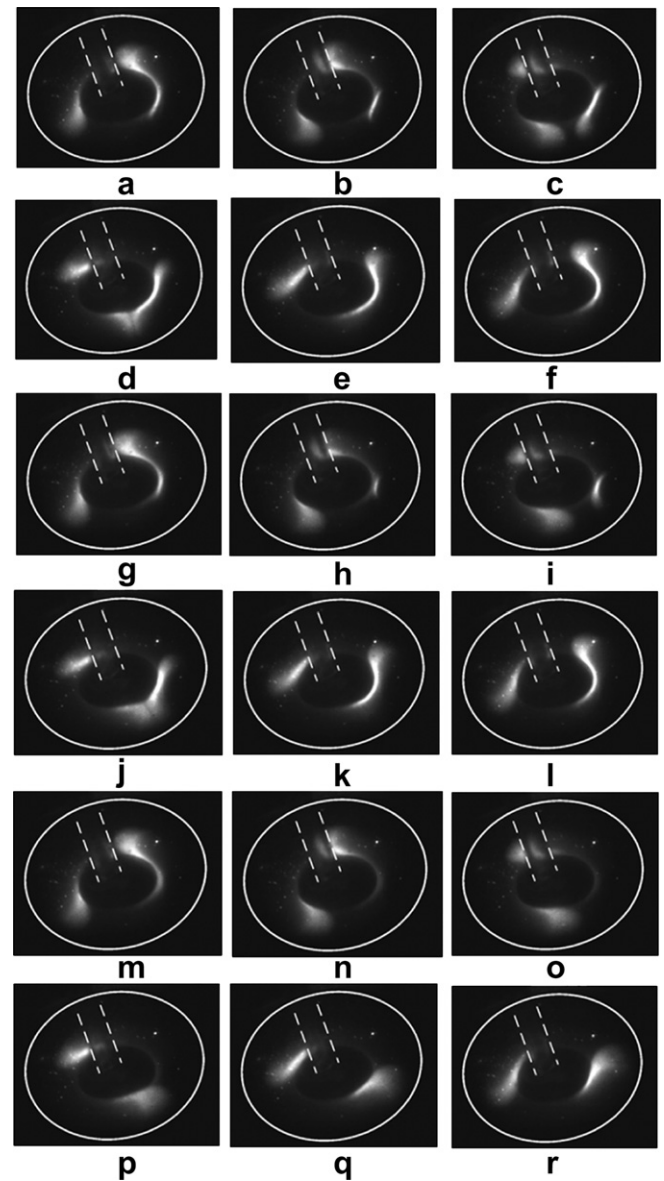
Fig. 4. Sequential frames of the transition process from a traveling flame to double Pelton-like flame. The gap distance of the radial channel $b = 2.0$ mm, inlet mixture velocity $V_{in} = 3.5$ m/s, and the mixture equivalence ratio φ was changed from 1.25 to 1.30.

3.2. Transition II: from a traveling flame to a double Pelton-like flame

In the radial micro-channel with a gap distance of 2.0 mm, we first set the parameters of the fresh mixture as: $V_{in} = 3.5$ m/s and $\varphi = 1.25$, and a traveling flame appeared. Then we increased the mixture equivalence ratio by 0.05 and the transition from the traveling flame to a double Pelton-like flame occurred. This transition process is illustrated in Fig. 4(a)–(r). From Fig. 4(a), it can be seen that the traveling flame front consists of one separate Pelton-like flamelet and another one which connects with a part of circular flame. The latter Pelton-like flamelet then separates from the circular flame front, as shown in Fig. 4(b). The remanent circular flame thus becomes very short. But it acts as an ignition source and the circular flame front grows increasing longer (Fig. 4(c)). Meanwhile, these Pelton-like flamelets rotate from one side of the circular flame front to the opposite. Finally, one of the Pelton-like

flamelet meets the circular flame front and they merge with each other (Fig. 4(d)). At the same time, a new outgrowth of Pelton-like flamelet appears at the other end of the circular flame front (Fig. 4(e) and (f)). At the moment of Fig. 4(f), a whole evolution process of the traveling flame accomplishes. From Fig. 4(g)–(l), the second cycle of the traveling flame finishes. However, during this cycle, the remanent circular flame front becomes even shorter, which is clearly seen in Fig. 4(h). From the moment of Fig. 4(m), the circular flame front gradually extinguishes (Fig. 4(m)–(o)) and the rotating double Pelton-like flame pattern forms (Fig. 4(p)–(r)).

3.3. Transition III: from a traveling flame to a single Pelton-like flame

Similarly as above, we first set $V_{in} = 4.0$ m/s and $\varphi = 1.25$, and a traveling flame occurred in the radial micro-channel with a gap distance of 2.0 mm. When the mixture equivalence ratio was
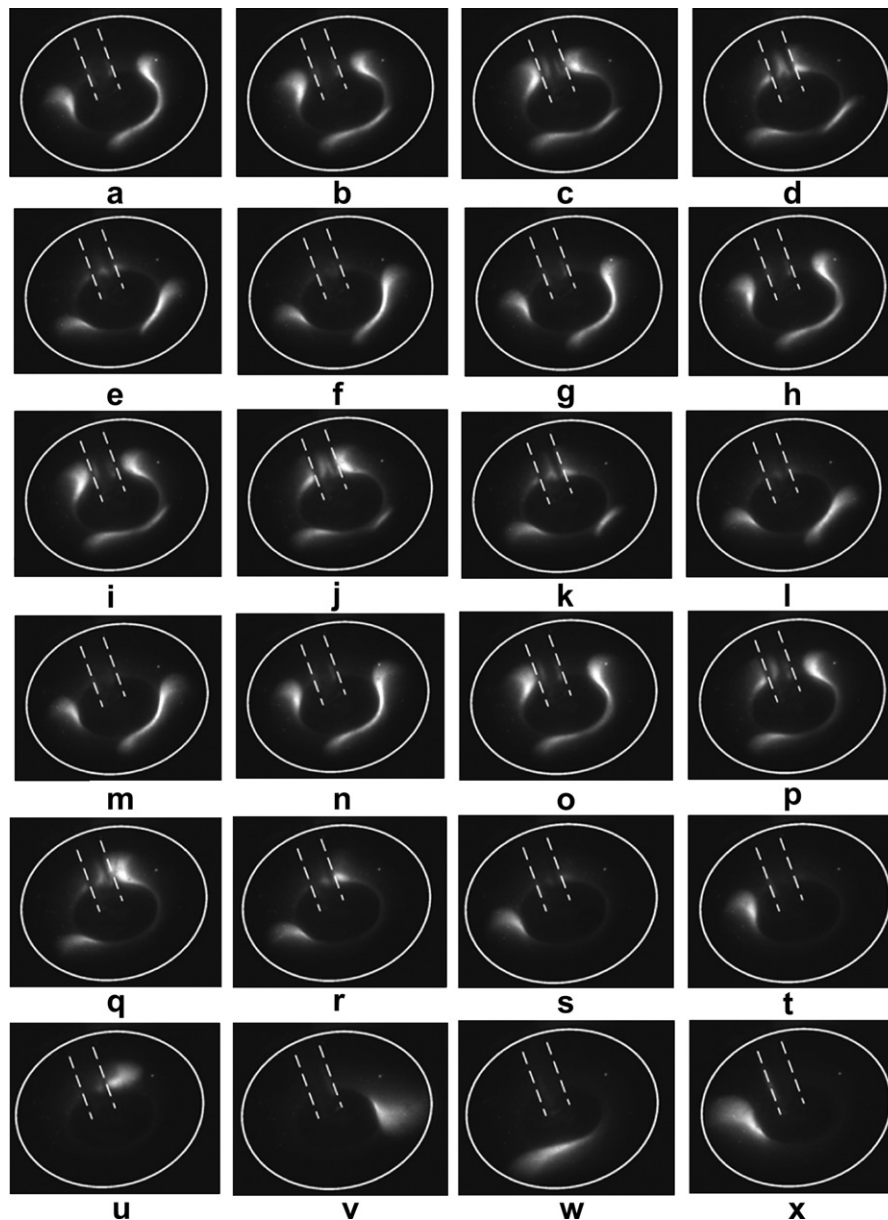
Fig. 5. Sequential frames of the transition process from traveling flame to single Pelton-like flame. The gap distance of the radial channel $b = 2.0$ mm, inlet mixture velocity $V_{in} = 3.5$ m/s, and the mixture equivalence ratio φ was changed from 1.25 to 1.30.

increased from 1.25 to 1.30, the transition from the traveling flame to a single Pelton-like flame took place, which is shown in Fig. 5(a)–(x).

From Fig. 5(a) and (b), it can be seen that the traveling flame front consists of one separate Pelton-like flamelet and a circular flame front which has two Pelton-like flamelets at its two ends. Then the two Pelton-like flamelets separate from the circular flame front (Fig. 5(c) and (d)). One of them meets the originally separate one and merge with each other (Fig. 5(d)–(f)). As a result, the two Pelton-like flamelets disappear (Fig. 5(f)). This extinction is somewhat like that of premixed counter flow flames under critical condition. As is also noticed in Fig. 5(d), the remanent circular flame front is very short. After that, it grows increasing longer (Fig. 5(e) and (f)). In Fig. 5(g) and (h), two new outgrowths of Pelton-like flamelets appear at the ends of the circular flame front. At the moment of Fig. 5(h), a whole evolution process of the traveling flame pattern accomplishes. From Fig. 5(i)–(n), the second cycle of the traveling flame finishes. However, during this cycle, the remanent circular flame front becomes even shorter, which is clearly seen in Fig. 5(j) and (k). From the moment of Fig. 5(o), the circular flame front gradually extinguishes (Fig. 5(o)–(q)). And after the mergence of the two Pleton-like flamelets which rotate in opposite directions, only the third Pelton-like flamelet survives (Fig. 5(r)–(t)) and remains its cyclic rotations (Fig. 5(t)–(x)).

3.4. Transition IV: from an unstable circular flame to a spiral-like flame

This transition was realized through an increase of the inlet mixture velocity in the radial micro-channel with a gap distance of 3.0 mm. We first obtained an unstable circular flame under the condition of $\varphi = 0.95$ and $V_{in} = 5.5$ m/s. Then, we increased the inlet mixture velocity to 6.0 m/s, a transition from an unstable circular flame to a spiral-like flame occurred. The whole process is recorded with the high-speed digital video camera and shown in Fig. 6(a)–(r).

From Fig. 6(a) it is noted that before the transition the flame front is an asymmetric circle with non-uniform luminosity. When the inlet mixture velocity was increased by 0.5 m/s, the flame front was pushed to locations of a larger radius, where the wall temperatures were higher than those of the original locations. The luminosity of the brighter part of the flame front grow even higher, as can be seen in Fig. 6(b) and (c). Then, local splitting of the bright half flame front occurred. The tips of the inner flame front ignited the unburned mixture in close vicinity to them, as shown in Fig. 6(d). Finally, the two tips connected with each other and form a new circular flame front which was slightly smaller than the original one (see Fig. 6(e) and (f)). The original outer flame front disappeared in the end due to the burnout of fuel and thus only one circular flame front remained (see Fig. 6(g) and (h)). Right after that, i.e., from Fig. 6(i) the unstable circular flame started to split again. But this time the splitting only took place at one location. The leading tip of the inner flame front ignited the unburned mixture close to it and consequently the rotating spiral-like flame formed, as can be clearly seen in Fig. 6(j). A whole rotating cycle is shown in Fig. 6(j)–(r).

4. Discussions

From our previous studies [31–33], it is seen that flame pattern formation in the heated narrow channel is a function of many factors, such as the mixture equivalence ratio, inlet velocity, channel gap, as well as the wall temperature level. But
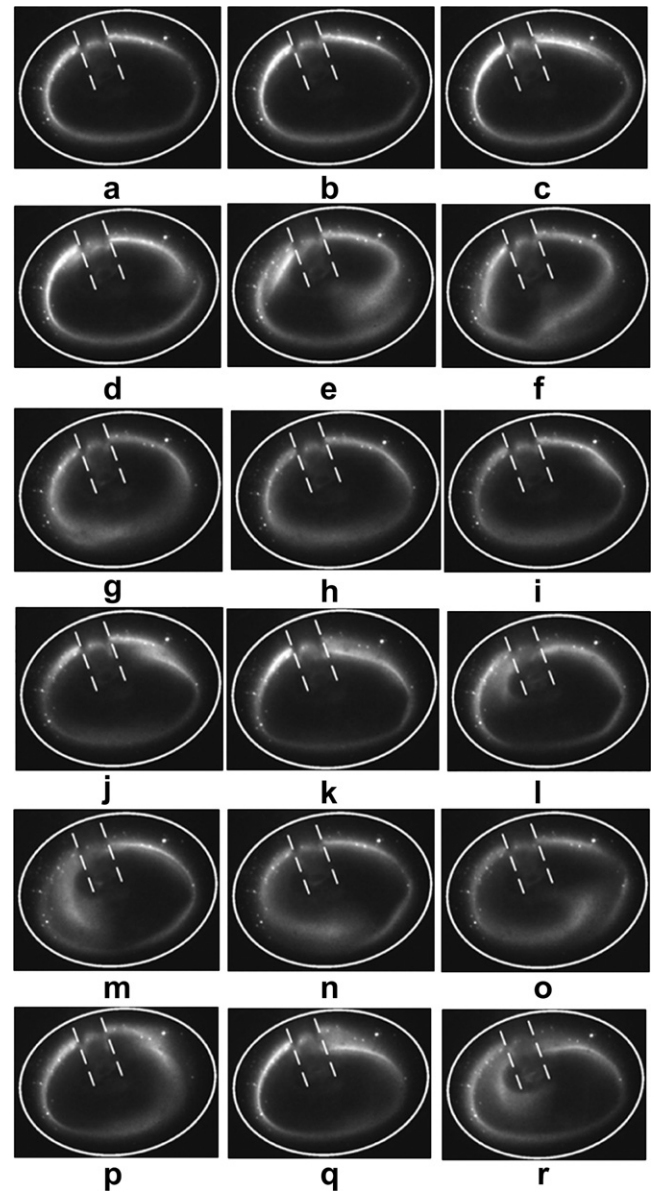
Fig. 6. Sequential frames of the transition process from an unstable circular flame to a spiral-like flame. The gap distance of the radial channel $b = 3.0$ mm, mixture equivalence ratio $\varphi = 0.95$, and the inlet mixture velocity V_{in} was changed from 5.5 to 6.0 m/s.

also, we can understand that those factors are not equally significant to each flame pattern. For example, we have investigated the effect of wall temperature level on flame pattern formations in the radial micro-channel [33]. The experimental results demonstrated that the Pelton-like flame and traveling flame are sensitive to the wall temperature level. In other words, traveling flame became circular flame, and Pelton-like flame became traveling flame at a higher wall temperature level. However, little improvement was achieved in the high inlet velocity region, i.e., the spiral-like flame was not stabilized by the higher wall temperature. These facts give us a hint that heat losses may be more important to the formations of Pelton-like flame and traveling flame, while flow instability might play a vital role in the pattern formation of the spiral-like flame. In the following we will discuss about the transition processes

which might provide more information on these flame pattern formations.

4.1. On the transitions from a stable circular flame to a traveling flame, and from a traveling flame to single and double Pelton-like flames

The movie recordings demonstrated that these transitions resulted from local extinction of the flame front, which is expected to be mainly caused by the unbalance between heat releases of the combustion reaction and heat losses from the flame to the wall. It is well known that heat release rate of a chemical reaction is proportional to the reaction rate, which is shown in Eq. (1) [34].

$$\varpi = \rho A Y_o^m Y_f^n \exp\left(-E/RT\right) \tag{1}$$

Here, A is a pre-exponential factor, Y_f and Y_o are mass fractions of the fuel and oxidizer, m and n are two constants, E is the activation energy and R is the universal gas constant, respectively.

From Eq. (1) one can see that the reaction rate is a function of the mass fractions of the fuel and oxidizer, i.e., the equivalence ratio of the pre-mixture. For a very rich CH_4/air mixture, its reaction rate decreases with the increase of the equivalence ratio. In other words, the heat release rate is reduced as the equivalence ratio is increased. Therefore, the balance between the heat release and heat losses will be broken, which leads to local extinction in the flame front. Thus, transitions from a stable circular flame to a traveling flame, and from a traveling flame to single and double Pelton-like flames occur.

4.2. On the transition from an unstable circular flame to a spiral-like flame

From the experimental results, we have already known that the transition form an unstable circular flame to a spiral-like flame was induced by local splitting in the flame front. To completely reveal the mechanisms of this dynamic process, simulating the combustion process with detailed chemistry is necessary. But as a first step, it is still of meaning to investigate the flow instability separately. As discussed above, flow instability may play an important role in the formation of the spiral-like flame. However, little attention has been paid to this effect in our previous studies. In Ref. [30], Kumar et al. assessed the role of buoyant forces based on a non-dimensional parameter Gr/Re^2 (ratio of buoyant to conventional forces) in the identical heated radial channel. The value of this parameter is very small (0.0001), which indicates that buoyant force does not play a significant role in the present experiment. Nevertheless, at relatively high inlet velocities, the impinging jet from the delivery tube may lead to an unstable flow field in the confined radial channel [35,36]. This will undoubtedly exert some effect on flame instability under high velocity condition.

For this, we performed numerical simulation of the isothermal flow field in the radial micro-channel using the CFD software package, Fluent 6.3. The maximal inlet velocity used in the experiments was 6.0 m/s, corresponding to a Reynolds number of ∼1542 in the delivery tube (in the radial channel, the maximal Reynolds number is much smaller due to the divergent radial flow). Although the geometry under investigation is axisymmetric, the flow field in the radial micro-channel might be asymmetric [35,36]. Therefore, three-dimensional, unstable, isothermal (i.e., heat transfer was not considered), incompressible, viscous fluid model was adopted in the numerical simulation. At the inlet of the radial channel, a fully developed velocity profile is adopted; while at the exit, an outflow boundary condition is set. To avoid the influence the recirculation flow at the outlet, we used a larger diameter (Ø60) as compared

with the one used in the experiment (Ø50). Both laminar and turbulent models have been tried in our simulations. The results demonstrated that general tendencies were similar. As two examples, Fig. 7(a) illustrates the pathlines in the vertical central plane when $b = 2.0$ mm and $V_{in} = 2.0$ m/s; while Fig. 7(b) shows the pathlines in the horizontal central plane when $b = 3.0$ mm and $V_{in} = 7.0$ m/s. The color of the path line represents the magnitude of flow velocity. Fig. 7 clearly demonstrates that when the inlet velocity and channel gap are small, the flow field in the radial channel is symmetric and steady. However, under conditions of large inlet velocity and channel gap, the flow field becomes asymmetric and unstable.

The flow field in the radial channel was also investigated by other researchers [35,36]. For example, Yoshimatsu and Mizushima [36] experimentally investigated on the instability and transition of radially outgoing flow between two parallel disks. Through flow visualization, they demonstrated that the flow was steady and symmetric at small Reynolds numbers, but became asymmetric above a critical Reynolds number. These works [35,36] qualitatively verifies our numerical simulations.

From Fig. 7(b) it can be clearly seen that, when the inlet velocity and channel gap are large, multiple vortices are formed. For example, a flow may be splitted into two, one moves upstream and forms a vortex, while the other is pushed downstream and forms another one. In the case of an unstable circular flame appearing in

b = 2.0 mm, V$_{in}$ = 2.0 m/s
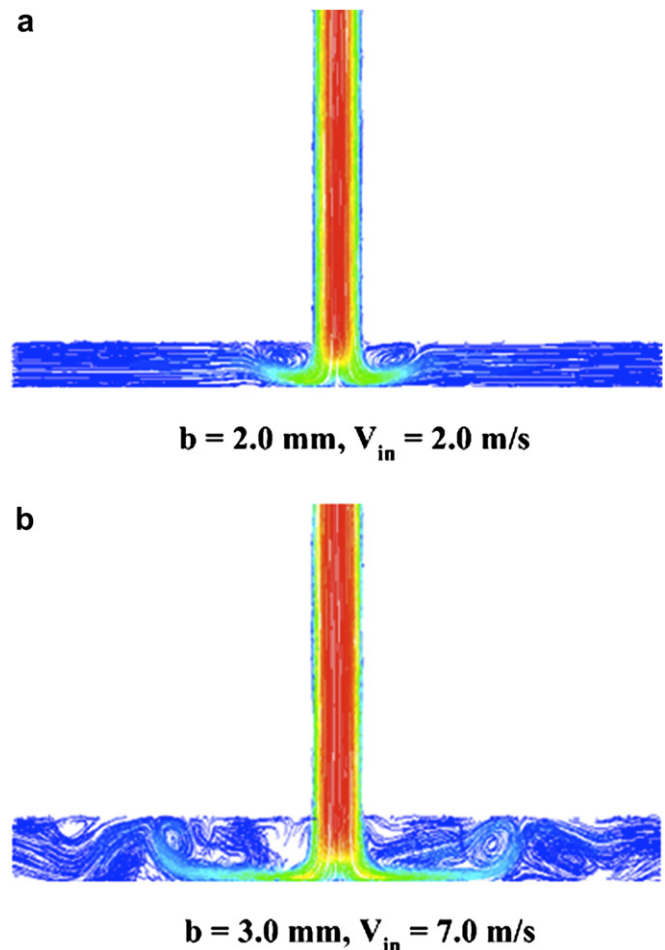
b = 3.0 mm, V$_{in}$ = 7.0 m/s

Fig. 7. Pathlines of the isothermal flow field in the radial channel under different conditions: (a) pathlines in the vertical central plane when $b = 2.0$ mm, $V_{in} = 2.0$ m/s; (b) pathlines in the vertical central plane when $b = 3.0$ mm, $V_{in} = 7.0$ m/s.

the radial channel, when the inlet velocity is suddenly increased to some extent, flow instability will also be intensified. Due to the unstable vortices, local splitting in the flame front will take place. The inner flame head then ignites the fresh mixture in the vicinity of it. As the tangential flow velocity is very small as compared with the burning velocity, the inner flame head will propagate in the circumferential direction at a relatively high speed. At the same time, it is noted that flame is quenched near the surface of the top disc when the gap distance is larger than 3.0 mm, which results in fuel leakage from this gap. Therefore, the outer flame front can survive after the splitting of the original flame front. Based on the above two reasons, the rotating spiral-like flame is formed.

5. Concluding remarks

Several flame pattern transitions of methane/air mixture were experimentally investigated in a radial channel with a gap distance of 2.0 and 3.0 mm. Those transitions were induced by a variation in the equivalence ratio or inlet velocity of the pre-mixture. From the movie recordings of those transition processes, one can see that local extinction of flame front is responsible for the transitions from a stable circular flame to a traveling flame, and from a traveling flame to single or double Pelton-like flames; while the transition from an unstable circular flame to a spiral-like flame was due to local splitting in the flame front and flame quenching near the surface of the top disc. Local extinction is expected to be a result of reduced heat release when the mixture equivalence ratio or inlet mixture velocity is changed. The possible underlying physics of local splitting of flame front is supposed to be resulted from the asymmetric and unstable flow field at large inlet velocities. Numerical simulation results verify that the isothermal flow field in the radial channel becomes asymmetric and unstable when the inlet velocity is sufficient high.

Acknowledgements

Nomenclature

A	pre-exponential factor
b	gap distance of the radial micro-channel, mm
E	activation energy
m	a constant in the chemical reaction rate formula
n	a constant in the chemical reaction rate formula
p	pressure, Pa
R	the universal gas constant
t	time, s
$\vec{u}$	velocity vector, m/s
V_{in}	inlet velocity at the delivery tube, m/s
Y_f	mass fraction of the fuel
Y_o	mass fraction of the oxidizer
φ	equivalence ratio
$\varnothing$	diameter, mm
ρ	density, kg/m^3
ν	kinematic viscosity, m^2/s

References

[1] D. Dunn-Rankin, E.M. Leal, D.C. Walther, Personal power systems, Progress in Energy and Combustion Science 31 (2005) 422–465.
[2] A.C. Fernadez-pello, Micro-power generation using combustion: issues and approaches, Proceedings of the Combustion Institute 29 (2002) 883–899.
[3] K. Maruta, Micro and mesoscale combustion, Proceedings of the Combustion Institute 33 (2011) 125–150.
[4] C.M. Spadaccini, A. Mehra, J. Lee, X. Zhang, S. Lukachko, I.A. Waitz, High power density silicon combustion system for micro gas turbine engines, Journal of Engineering for Gas Turbines and Power 125 (2003) 709–719.
[5] V. Zamashchikov, Experimental investigation of gas combustion regimes in narrow tubes, Combustion and Flame 108 (1997) 357–359.
[6] T.T. Leach, C.P. Cadou, The role of structural heat exchange and heat loss in the design of efficient silicon micro-combustors, Proceedings of the Combustion Institute 30 (2005) 2437–2444.
[7] S. Raimondeau, D. Norton, D.G. Vlachos, R.I. Masel, Modeling of high-temperature microburners, Proceedings of the Combustion Institute 29 (2002) 901–907.
[8] S.A. Lloyd, F.J. Weinberg, A burner for mixtures of very low heat content, Nature 251 (1974) 47–48.
[9] P.D. Ronney, Analysis of non-adiabatic heat recirculating combustors, Combustion and Flame 135 (2003) 421–439.
[10] C.H. Kuo, P.D. Ronney, Numerical modeling of non-adiabatic heat-recirculating combustors, Proceedings of the Combustion Institute 31 (2007) 3277–3284.
[11] N.I. Kim, S. Kato, T. Kataoka, T. Yokomori, S. Maruyama, T. Fujimori, K. Maruta, Flame stabilization and emission of small Swiss-roll combustors as heaters, Combustion and Flame 141 (2005) 229–240.
[12] N.I. Kim, S. Aizumi, T. Yokomori, S. Kato, T. Fujimori, K. Maruta, Development and scale effects of small Swiss-roll combustors, Proceedings of the Combustion Institute 31 (2007) 3243–3250.
[13] W.M. Yang, S.K. Chou, C. Shu, Z.W. Li, H. Xue, Combustion in micro-cylindrical combustors with and without a backward facing step, Applied Thermal Engineering 22 (2002) 1777–1787.
[14] L.Q. Jiang, D.Q. Zhao, X.H. Wang, W.B. Yang, Development of a self-thermal insulation miniature combustor, Energy Conversion and Management 50 (2009) 1308–1313.
[15] J.W. Li, B.J. Zhong, Experimental investigation on heat loss and combustion in methane/oxygen micro-tube combustor, Applied Thermal Engineering 28 (2008) 707–716.
[16] B. Khandelwal, S. Kumar, Experimental investigations on flame stabilization behavior in a diverging micro channel with premixed methane-air mixtures, Applied Thermal Engineering 30 (2010) 2718–2723.
[17] K. Maruta, J.K. Parc, K.C. Oh, T. Fujimori, S.S. Minaev, R.V. Fursenko, Characteristics of microscale combustion in a narrow heated channel, Combustion, Explosion and Shock Waves 40 (2004) 516–523.
[18] K. Maruta, T. Kataoka, N.I. Kim, S. Minaev, R. Fursenko, Characteristics of combustion in a narrow channel with a temperature gradient, Proceedings of the Combustion Institute 30 (2005) 2429–2436.
[19] S. Minaev, K. Maruta, R. Fursenko, Nonlinear dynamics of flame in a narrow channel with a temperature gradient, Combustion Theory and Modeling 11 (2007) 187–203.
[20] F. Richecoeur, D.C. Kyritsis, Experimental study of flame stabilization in low Reynolds and Dean number flows in curved mesoscale ducts, Proceedings of the Combustion Institute 30 (2005) 2419–2427.
[21] Y. Fan, Y. Suzuki, N. Kasagi, Experimental study of micro-scale premixed flame in quartz channels, Proceedings of the Combustion Institute 32 (2009) 3083–3090.
[22] Y. Fan, Y. Suzuki, N. Kasagi, Quenching mechanism study of oscillating flame in micro channels using phase-locked OH-PLIF, Proceedings of the Combustion Institute 33 (2011) 3267–3273.
[23] T.L. Jackson, J. Buckmaster, Z. Lu, D.C. Kyritsis, L. Massa, Flames in narrow circular tubes, Proceedings of the Combustion Institute 31 (2007) 955–962.
[24] G. Pizza, C.E. Frouzakis, J. Mantzaras, A.G. Tomboulides, K. Boulouchos, Dynamics of premixed hydrogen/air flames in micro-channels, Combustion and Flame 152 (2008) 433–450.
[25] G. Pizza, C.E. Frouzakis, J. Mantzaras, A.G. Tomboulides, K. Boulouchos, Dynamics of premixed flames in a narrow channel with a step-wise wall temperature, Combustion and Flame 155 (2008) 2–20.
[26] S.S. Minaev, E.V. Sereshchenko, R.V. Fursenko, A.W. Fan, K. Maruta, Splitting flames in a narrow channel with a temperature gradient in the walls, Combustion, Explosion and Shock Waves 45 (2009) 119–125.
[27] A.W. Fan, S.S. Minaev, E. Sereshchenko, Y. Tsuboi, H. Oshibe, H. Nakamura, K. Maruta, Dynamic behavior of splitting flames in a heated channel, Combustion, Explosion and Shock Waves 45 (2009) 245–250.
[28] S. Kumar, K. Maruta, S. Minaev, Pattern formation of flames in radial micro-channels with lean methane-air mixtures, Physical Review E 75 (2007) 016208.
[29] S. Kumar, K. Maruta, S. Minaev, On the formation of multiple rotating Pleton-like flame structures in radial micro-channels with lean methane-air mixtures, Proceedings of the Combustion Institute 31 (2007) 3261–3268.

[30] S. Kumar, K. Maruta, S.S. Minaev, Appearance of target pattern and spiral flames in radial micro-channels with CH_4-air mixtures, Physics of Fluids 20 (2008) 024101.

[31] A.W. Fan, S. Minaev, E.V. Sereshchenko, R.V. Fursenko, S. Kumar, W. Liu, K. Maruta, Experimental and numerical investigations of flame pattern formation in a radial micro-channel, Proceedings of the Combustion Institute 32 (2009) 3059–3066.

[32] A.W. Fan, S. Minaev, S. Kumar, W. Liu, K. Maruta, Regime diagrams and characteristics of flame patterns in radial micro-channels with temperature gradients, Combustion and Flame 153 (2008) 479–489.

[33] A.W. Fan, S. Minaev, S. Kumar, W. Liu, K. Maruta, Experimental study on flame pattern formation and combustion completeness in a radial micro-channel, Journal of Micromechanics and Microengineering 17 (2007) 2398–2406.

[34] S.R. Turns, An Introduction to Combustion, second ed. McGRAW-Hill, New York, 2000.

[35] A. Chatterjee, Multiple vortex formation in steady laminar axisymmetric impinging flow, Computers and Fluids 37 (2008) 1061–1076.

[36] K. Yoshimatsu, J. Mizushima, Symmetry breaking of radially outgoing flow between two parallel disks, Journal of Physical Society of Japan 72 (2003) 3028–3031.